Journal of Photochemistry, 2 (1973/74) 255–266

A COMPUTER SIMULATION OF PHASE-SHIFT MEASUREMENTS OF THE QUENCHING AND TRAPPING OF RESONANCE RADIATION AT LARGE OPTICAL DEPTHS

LEON F. PHILLIPS
Chemistry Department, University of Canterbury, Christchurch (New Zealand)
(Received May 15, 1973)

SUMMARY

Numerical calculations of the build-up and decay of fluorescence have been made for a model system in which the rate of internal radiative transfer to a point is governed by the average concentration of excited species in the immediate neighbourhood of that point. This corresponds to the limit of very large optical depth. The concentration of excited species has been evaluated as a function of time at each point on a cubical grid, for grids having 5, 9, 13, 17, or 21 equally-spaced points along each axis. The phase and amplitude of the fluorescence signal have been calculated for various quencher concentrations, modulation frequencies, and points of observation. The radiation trapping time characteristic of the quenching of steady-state fluorescence differed from that calculated from the phase delay between the fundamental components of exciting radiation and fluorescence. Trapping times, T, derived from phase-shifts obtained at different quenching rates obeyed the equation:

$$T_0/T = 1 + Q\,T_0$$

at small Q values, where Q is the pseudo first-order rate constant of the quenching process and T_0 is the trapping time measured in absence of quencher.

INTRODUCTION

The theoretical problem of the trapping of resonance radiation has been investigated analytically[1–3] and numerically[4] in relation to both the quenching of steady-state fluorescence and the rate of decay of fluorescence after pulsed excitation. Exact results have been obtained for systems with natural, Doppler, and Lorentz broadening of the resonance line[5], at large and intermediate optical depths. Van Volkenburgh and Carrington[4] have shown that in the presence of radiation trapping the Stern–Volmer equation for quenching of steady-state fluorescence becomes:

$$F_0/F = 1 + k_Q N_Q/gA = 1 + Q/gA \tag{1}$$

where F_0 and F are the unquenched and quenched fluorescence intensities, k_Q is the rate constant for quenching by a quencher whose concentration is N_Q molecules/cm^3, A is the Einstein coefficient for spontaneous emission of the resonance line, and g is an escape factor which depends on the concentration of ground state fluorescers and the geometry of the system. Following Holstein[1], they expressed the intensity of emission subsequent to pulsed excitation as a sum of exponential terms:

$$F = \sum_n F_n \exp(-\beta_n t) \tag{2}$$

where the relative magnitudes of the coefficients F_n were also found to depend on system geometry and fluorescer concentration. At a sufficiently long time after the initial excitation pulse the series in eqn. (2) can be approximated by the term corresponding to the lowest decay mode:

$$F = F_1 \exp(-\beta_1 t) \tag{3}$$

where $\beta_1 = hA$ (4)

and h is another escape factor, different from g. In the presence of a quencher eqn. (3) becomes

$$F = F_1 \exp[-(Q + hA)\, t] \tag{5}$$

with Q as defined in eqn. (1).

Radiation trapping times characteristic of the system are defined by:

$$T_0' = 1/gA \tag{6}$$

and $T_0'' = 1/hA$ (7)

If the fluorescence system is excited periodically by a signal of the form

$$I(t) = \sum_n I_n \sin n\omega t \tag{8}$$

where $\omega = 2\pi f$ is the fundamental chopping frequency in rad/s, the fluorescent intensity will be given by an expression of the form:

$$F(t) = \sum_n F_n \sin(n\omega t - \delta_n) \tag{9}$$

where the δ_n are phase delays between the various Fourier components of the exciting radiation and the fluorescence[6]. These phase-shifts define a further trapping time T_0, such that:

$$\tan \delta_n = 2\pi n f T_0 \tag{10}$$

As with the other trapping times, T_0 tends to the natural lifetime $\tau_0 = 1/A$ as the optical density tends to zero.

In a study of the quenching and trapping of Lyman-α radiation at large optical depths[7] some rate constants for quenching of H(^{2}P) were estimated from measurements of phase angles and fluorescence amplitudes as a function of quencher concentration, on the assumption that T_0 was approximately equal to T_0'. The rate constants so obtained were on the low side, and the results indicated that T_0 and T_0' might differ by as much as a factor of 2. The rate constants were evaluated from the Stern–Volmer equation written in the form:

$$T_0/T = 1 + k_Q N_Q T_0 \tag{11}$$

An extrapolation procedure was used to determine the phase angle corresponding to zero phase shift and, because of the scatter of the phase-shift data, T_0 on the right-hand side of eqn. (11) was set equal to T_0'. More recently a phase-shift study of the quenching and trapping of Cd 228.8 nm resonance radiation at large optical depths[8] has yielded results which are sufficiently precise to allow the use of eqn. (11) without the assumption that $T_0' \sim T_0$. In view of the wide potential applicability of this approach for determining quenching rates it appears advisable to obtain some theoretical justification for eqn. (11), with particular reference to the type of experimental system which was employed in the Lyman-α and Cd 228.8 nm studies. The present paper, which describes a computer simulation of the build-up and decay of fluorescence at the limit of very large optical depth, represents a first step in this direction.

THEORY

The time variation of the concentration of excited species $U(\mathbf{r})$ at a point defined by the vector $\mathbf{r}$ is given by[1]:

$$\mathrm{d}U(\mathbf{r})/\mathrm{d}t = I_{\mathrm{abs}}(\mathbf{r}) - (A + Q)\, U(\mathbf{r}) + \int_0^\infty A.\, U(\mathbf{r}').G(\mathbf{r},\mathbf{r}')\, \mathrm{d}\mathbf{r}' \tag{12}$$

In eqn. (12) $I_{\mathrm{abs}}(\mathbf{r})$ is the rate of absorption of the exciting radiation at $\mathbf{r}$, $(A + Q)\, U(\mathbf{r})$ is the rate of loss of excited species by quenching and radiation, and the last term on the right-hand side represents the rate of radiative transfer to $\mathbf{r}$ from all points $\mathbf{r}'$. The quantity $G(\mathbf{r},\mathbf{r}')$ gives the probability that a photon emitted at $\mathbf{r}'$ will be absorbed at $\mathbf{r}$ (and *vice versa*). To simplify the notation we now transfer the origin to point $\mathbf{r}$, replace $\mathbf{r}' = \mathbf{r}$ by $\mathbf{x}$, and replace $G(\mathbf{r},\mathbf{r}')$ by $G(x)$, $I_{\mathrm{abs}}(\mathbf{r})$ by I_{abs}, $U(\mathbf{r})$ and $U(\mathbf{r}')$ by U and $U(x)$ respectively. If the probability of transmission of a photon a distance $x = |\mathbf{x}|$ is $P(x)$, then

$$G(x) = -\mathrm{d}P(x)/\mathrm{d}x \tag{13}$$

The main difficulties associated with solving eqn. (12) result from the problem of evaluating $P(x)$ for different forms of emission and absorption line, and the evaluation of the transfer integral for the appropriate boundary conditions. Once

$U(\mathbf{x})$ is known for all x at a given time the intensity of emission in any direction can be calculated from the integral of $A.U(\mathbf{x}).P(x)$ along the line of sight.

At large optical depths the value of $P(x)$ falls off very quickly with increasing x. For example, for the Cd 228.8 nm line, with a peak Doppler-only absorption coefficient of 1120 cm^{-1} and assuming natural plus Doppler broadening, the values of $P(x)$ shown in Table 1 are obtained[5]. Thus, if the fluorescence cell is large enough for $U(\mathbf{x})$ to be a slowly-varying function of $\mathbf{x}$, it is reasonable to substitute for $U(\mathbf{x})$ inside the integral a mean concentration of excited species $U(x)$ at the distance x from the origin. The transfer term then becomes

$$A\int_0^\infty U(x)\, G(x)\, \mathrm{d}x \tag{14}$$

where $U(x)$ is to be obtained by averaging over a spherical shell of radius x. (There is no factor of 4π because the volume of the shell increases with increasing x at the same rate as the solid angle subtended by an element of volume at the origin decreases with increasing x.) In the limit of very large optical depth we may further average $U(x)$ to obtain $\bar{U}$, the mean concentration of excited species in the neighbourhood of the point under consideration. The transfer term then simplifies to:

$$\begin{aligned} A\bar{U}\int_0^\infty G(x)\mathrm{d}x &= -A\bar{U}\int_0^\infty \frac{\mathrm{d}P(x)}{\mathrm{d}x}\,\mathrm{d}x \\ &= -A\bar{U}\,(P(\infty)-P(0)) = A\bar{U} \end{aligned} \tag{15}$$

and eqn. (12) becomes:

$$\mathrm{d}U/\mathrm{d}t = I_{\mathrm{abs}} - (A + Q)U + A\bar{U} \tag{16}$$

TABLE 1

TRANSMISSION PROBABILITY $P(x)$ FOR Cd 228.8 nm RESONANCE RADIATION IN A SYSTEM WITH NATURAL PLUS DOPPLER BROADENING, AND A PEAK DOPPLER-ONLY ABSORPTION COEFFICIENT OF 1120 cm^{-1}

x (cm)	$P(x)$
0.0	1.0
0.00089	0.533
0.00357	0.140
0.00804	0.0539
0.0223	0.0211
0.04375	0.0123
0.108	0.00736
0.514	0.00397
1.032	0.00254
1.808	0.00168

With I_{abs}, dU/dt, and Q all set equal to zero eqn. (16) reduces to the condition for thermal equilibrium in a large enclosure. Equation (16) is the basis of the calculation described here. For a finite time interval Δt during which $\overline{U}$ is assumed constant this equation can be integrated to yield:

$$U(t + \Delta t) = U(t) + \left\{(I_{abs} + A\overline{U})/(A + Q) - U(t)\right\} \times \left\{1 - \exp\left[-(A + Q)\,\Delta t\right]\right\} \quad (17)$$

which is in a form suitable for the evaluation of U as a function of t with a digital computer.

A diagram of the model system used in the calculations is shown in Fig. 1. It was intended to simulate a fluorescence cell consisting of two Woods horns joined at right angles, with one horn facing the exciting beam and the other the spectrometer slit. Because the microwave-powered lamps used in our phase-shift measurements produce a very broad emission line the value of I_{abs} (z) was calculated as a function of z, the distance along the vertical axis, as if light were being absorbed from a continuous source. This meant that the wings of the absorption line, where Doppler broadening predominates, produced the major contribution to I_{abs} in the interior of the cell. Relative values of I_{abs} so obtained are given in Table 2. The cell was divided by a cubical grid, the number of points along a side being chosen to be 5, 9, 13, 17, or (in a few calculations) 21. For grid points which lay outside the path of the exciting beam I_{abs} was always zero. For points inside the exciting beam I_{abs} during the first half of a chopping cycle was set equal to the appropriate relative value, obtained as for Table 2, multiplied by 10^{15}. During the second half of the cycle I_{abs} was zero everywhere. This corresponds to square-wave excitation, which is a close approximation to that used experimentally. The value of A (5×10^8 s^{-1}) was chosen to correspond to the Cd 228.8 nm system. At the beginning of a cycle U was set equal to zero at every

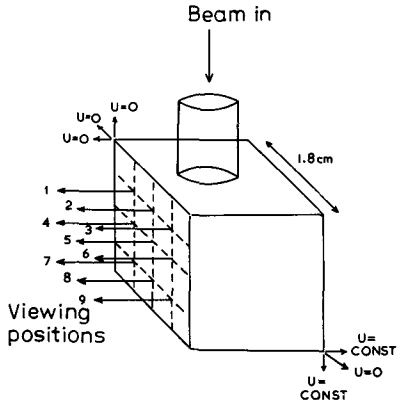

Fig. 1. Model used to simulate the behaviour of the fluorescence system.

TABLE 2

RELATIVE RATES OF LIGHT ABSORPTION FROM A CONTINUUM SOURCE AS A FUNCTION OF z (PEAK DOPPLER-ONLY ABSORPTION COEFFICIENT = 1120 cm^{-1}, RATIO NATURAL TO DOPPLER BROADENING = 0.038)

z (cm)	$I_{abs}(z)$
0.0	1.00000
0.225	0.00658
0.450	0.00475
0.675	0.00369
0.900	0.00303
1.125	0.00257
1.350	0.00225
1.575	0.00199
1.800	0.00179

grid point. Then, starting at the centre of the face of the cell through which the exciting beam entered, U was evaluated from eqn. (17) for a time interval Δt equal to one-thousandth of the duration of a chopping cycle. U was evaluated first along a line at right angles to the viewing direction (z axis), then along parallel lines at the same z value in a progression towards the back of the cell, then finally at the same z value along parallel lines between the centre and the front of the cell. The process was then repeated for the set of grid points at the next z value, and so on. At each grid point $\overline{U}$ was obtained by averaging over the U values existing at the six surrounding grid points. For a grid point on a face of the cell the contribution to $\overline{U}$ from any surrounding point outside the cell was zero, while for surrounding points which were also on the cell face the contribution to $\overline{U}$ was halved. In evaluating $\overline{U}$ for a grid point adjacent to one of the two Woods horns the concentration at the surrounding point inside the horn was set equal to the concentration at the grid point itself. Once U had been evaluated for each grid point at time Δt the emission observed at each of the nine viewing positions shown in Fig. 1 was calculated assuming a pure Doppler line, using Gauss–Hermite quadrature, and stored. The whole process was then repeated for time $2\Delta t$, and so on to the end of the chopping cycle. U was actually calculated at only half the grid points, values at the other half being fixed by symmetry. The chopping frequency (75 to 3000 kHz) was normally chosen to be low enough so that the emission intensity reached its steady-state value during both halves of the cycle, which meant that data from a single cycle would provide the information required for a Fourier analysis. The amplitudes and phases of the fundamental components of the output signals were calculated from the formulae:

$$a = \sum_{m=1}^{1000} F(m.\Delta t) \sin(2\pi m/1000) \tag{18}$$

$$b = \sum_{m=1}^{1000} F(m.\Delta t) \cos(2\pi m/1000) \tag{19}$$

the amplitude being given by:

$$|F| = (a_1^2 + b_1^2)^{1/2} \tag{20}$$

and the phase shift by:

$$\delta = \tan^{-1}(b/a) + \pi/2 \tag{21}$$

RESULTS

The results obtained are expected to depend on the number of grid points used, since this governs the size of the region over which U is averaged to obtain $\overline{U}$. Also, any change in the value of I_{abs} in the path of the beam will take a number of time increments to affect the whole grid system, one time increment being required for the disturbance to propagate past each grid point, and this will lead to error which will be most significant for small phase angles. Because of this effect, which is here termed the "propagation delay", it is not necessarily an advantage to use a large number of grid points, even though a larger number would be likely to give a better approximation to the final steady-state distribution of U. Figure 2 shows the variation of the steady-state value of U with distance from the front face of the cell at viewing positions 2 and 8 (see Fig. 1) for 5, 9, 13, and 17 grid points, with $Q = 0$. Figure 3 shows analogous results for $Q = A/20$. In general it is found that there is a fairly marked change in the calculated U distribution on going from 5 to 9 grid points, with smaller changes on going from 9 to 13 and 13 to 17. Since the amount of computer time required varies approximately as the cube of the number of grid points, most calculations were performed for a $9 \times 9 \times 9$ grid. Useful comparisons could be made only between calculations based on the same number of grid points. The typical variation of the phase shift with the number of grid points is shown in Table 3.

A test of eqn. (10) for a $9 \times 9 \times 9$ grid is shown in Fig. 4, where the tangent of the phase shift with $Q = A/20$ is plotted as a function of frequency for three viewing positions. At low frequencies the calculated phase shift is too large because of the "propagation delay" effect, while the points for a frequency of 3 MHz also deviate from the line, possibly because at this frequency the intensity was significantly greater than zero at the end of the cycle, with the result that the Fourier analysis is slightly in error. Figure 4 also demonstrates the manner in which the phase shift varies with viewing position. As the results in Table 3 show, the variation is much less marked in the direction at right angles to the exciting beam than it is parallel to the beam. The experimental implication of this result is that a spectrometer slit should preferably be aligned at right angles to the exciting

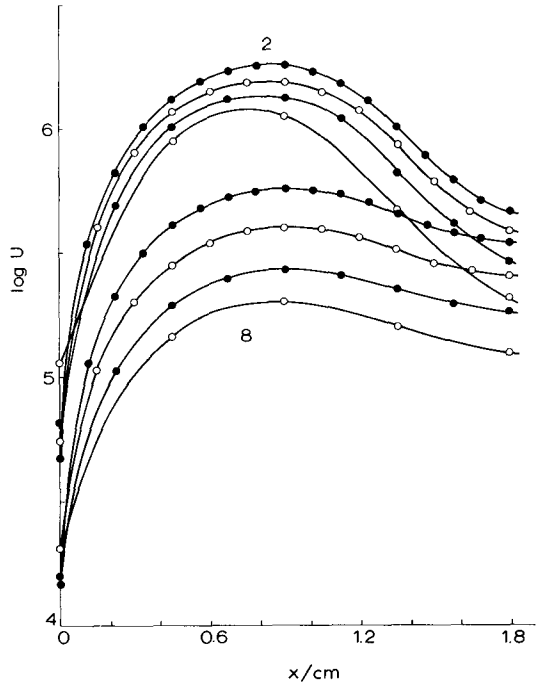

Fig. 2. Effect of the number of grid points on the calculated steady-state concentration of excited species along the line of sight from the viewing position to the rear of the cell, for viewing positions 2 and 8 (see Fig. 1). Upper curves for position 2, lower for position 8. $Q = 0$.

TABLE 3

VARIATION OF PHASE ANGLE (DEGREES) WITH NUMBER OF GRID POINTS AND VIEWING POSITION, $Q = A/20, f = 600$ kHz

Viewing position	Number of grid points			
	5 × 5 × 5	9 × 9 × 9	13 × 13 × 13	17 × 17 × 17
1,3	2.022	4.223	6.536	8.808
2	1.669	4.105	6.415	8.582
4,6	2.852	6.534	9.195	10.538
5	2.642	6.414	8.950	10.042
7,9	3.839	7.756	8.700	9.251
8	3.681	7.429	8.307	8.809

beam, not parallel with it, especially if the viewing position is close to the point of entry of the exciting beam.

The Stern–Volmer equation for steady-state fluorescence intensities can be written in the form:

$$F_0/F = 1 + QT_0' = 1 + \frac{Q}{A}(AT_0') \tag{22}$$

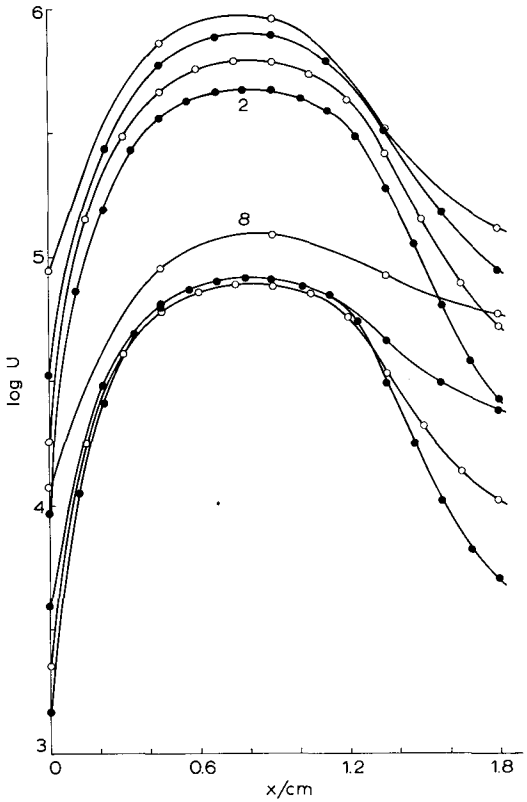

Fig. 3. As in Fig. 2, but $Q = A/20$.

A test of this equation for the $9 \times 9 \times 9$ grid is shown in Fig. 5, where F_0 is the amplitude of the signal for $Q = 0$, as given by eqn. (20). The form of the results is seen to be consistent with eqn. (22) provided F_0/F is not too large. The slopes of the lines in Fig. 5 can be combined with the value of A (5×10^8 s^{-1}) to give T_0' values of 32, 61, and 90 ns, at the three viewing positions.

Equation (11) can similarly be written in the form:

$$1/T = 1/T_0 + \left(\frac{Q}{A}\right) A \tag{23}$$

A test of this result is shown in Fig. 6, where the points indicate reciprocal trapping times calculated for the $9 \times 9 \times 9$ grid and the lines are drawn with slope equal to A through the points corresponding to values of $1/T_0$. The points are seen to deviate from the theoretical lines at large values of Q, the deviation being more pronounced at greater distances from the point of entry of the exciting beam. At Q/A values below about 0.01 the agreement is seen to be reasonably satisfactory at all three viewing positions. The T_0 values obtained from the phase shifts at $Q = 0$ are 30, 54, and 77 ns in viewing positions 2, 5 and 8, respectively. Thus the

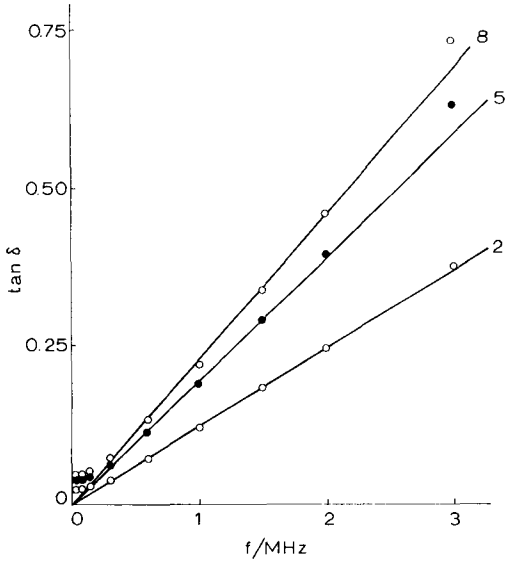

Fig. 4. Variation with frequency of the phase shift observed at viewing positions 2, 5 and 8, $Q = A/20$, 9 × 9 × 9 grid.

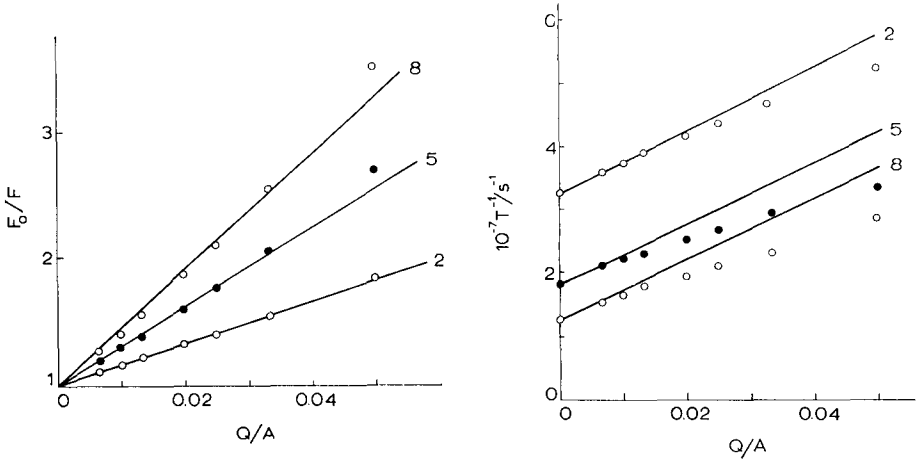

Fig. 5. Test of eqn. (22) for viewing positions 2, 5 and 8. (Various modulation frequencies, 9 × 9 × 9 grid.)

Fig. 6. Test of eqn. (23) for viewing positions 2, 5 and 8. (500 kHz, 9 × 9 × 9 grid.)

difference between T_0 and T_0' is also found to increase with increasing distance from the point of entry of the exciting beam. Similar conclusions can be drawn from the analogous results for a 13 × 13 × 13 grid, for which the deviations from the expected straight lines at high Q/A values are slightly greater. At least in part

these deviations are associated with errors arising from the propagation delay, which are most serious at small phase angles.

An additional phenomenon which enters into quenching measurements in the type of system we are considering is Lorentz broadening of the absorption and emission lines of the fluorescer by the added quencher. With the present model system the only effect of this broadening is to alter the rate of absorption I_{abs} in the body of the cell where absorption from the continuum source occurs mainly in the wings of the absorption line. To test the importance of this effect some calculations were made in which the ratio of natural to Doppler broadening was replaced by a quantity α given by:

$$\alpha = (\Delta\nu_N + \Delta\nu_L)/\Delta\nu_D \tag{24}$$

where $\Delta\nu_N$ and $\Delta\nu_D$ were 8×10^7 and $21 \times 10^8\ s^{-1}$, respectively (values appropriate for the Cd 228.8 nm resonance line at 550 K), and $\Delta\nu_L$ was calculated from the formula given by Mitchell and Zemansky[5] assuming a reduced mass of 22 amu and a typical collision-broadening cross-section of $6 \times 10^{-15}\ cm^2$. The value of N_Q was calculated for $k_Q = 10^{-10}\ cm^3\ molecule^{-1}\ s^{-1}$. Results for Q equal to $A/20$ and $A/30$ are shown in Table 4 for pure Doppler broadening, Doppler plus

TABLE 4

EFFECT OF NATURAL AND LORENTZ BROADENING ON CALCULATED PHASE SHIFTS AND AMPLITUDES $\sigma_L^2 = 6 \times 10^{-15}\ cm^2$, $k_Q = 10^{-10}\ cm^3\ molecule^{-1}\ s^{-1}$, $A = 5 \times 10^8\ s^{-1}$, $9 \times 9 \times 9$ grid viewing positions 2, 5, 8, units of $F = 10^{10}$ photon/s, units of δ = degrees

Broadening type	α	Q/A	δ_2	δ_5	δ_8	F_2	F_5	F_8
Doppler only	0.0	0.05	4.122	6.681	8.109	2.267	0.6031	0.2042
Doppler + natural	0.038	0.05	4.105	6.414	7.429	2.399	0.7002	0.2705
Lorentz added	0.091	0.05	4.091	6.308	7.299	2.483	0.7484	0.2933
Doppler only	0.0	0.025	5.011	8.512	11.501	3.025	0.9568	0.3537
Doppler + natural	0.038	0.025	5.010	8.196	10.446	3.228	1.123	0.4759
Lorentz added	0.061	0.025	5.006	8.130	10.314	3.291	1.165	0.5008

natural broadening, and Doppler plus both natural and Lorentz broadening. It is apparent that the addition of Lorentz broadening has a significant effect on the amplitudes, but very little effect on the phase angles. For the value of k_Q chosen here $Q = A/20$ corresponds to $N_Q = 2.5 \times 10^{17}$ molecule/cm^3, or about 10 Torr of quencher. Thus for partial pressures of quencher equal to 1 Torr or less the effect of Lorentz broadening on phase-shift measurements should be completely negligible.

CONCLUSIONS

The absolute values of phase shifts obtained from these calculations are not expected to be significant because the propagation delay effect necessitates working with a rather small number of grid points. The errors due to this effect could no doubt be reduced by increasing the number of time increments per cycle (initial calculations made with 100 increments instead of 1000 show the advantage of doing so), but even for a $9 \times 9 \times 9$ grid the additional cost in terms of computer time would be excessive, especially since significant qualitative conclusions can be drawn from the present results. These conclusions are:

(1) Phase-shift measurements of atomic resonance radiation at large optical depths are capable of yielding rate constants for quenching reactions through the application of eqn. (11). Care is necessary, however, to avoid errors due to the variation of phase angle with distance from the point of entry of the exciting beam.

(2) The radiation trapping time calculated from the phase shift observed between exciting radiation and fluorescence in the absence of quencher is not the same as the trapping time which is characteristic of the quenching of steady-state fluorescence.

(3) Lorentz broadening has a smaller effect on the phase shift observed in the presence of a quencher than on the intensity of steady-state fluorescence.

ACKNOWLEDGEMENTS

This work was supported by the New Zealand Universities Research Committee and by Grant AF-AFOSR-71-2134 from the United States Air Force Office of Scientific Research.

REFERENCES

1 T. Holstein, *Phys. Rev.*, 72 (1947) 1212.
2 P. J. Walsh, *Phys. Rev.*, 116 (1959) 511.
3 C. van Trigt, *Phys. Rev.*, 181 (1969) 97.
4 G. Van Volkenburgh and T. Carrington, *J. Quant. Spectros. Radiat. Trans.*, 11 (1971) 1181.
5 A.C.G. Mitchell and M. W. Zemansky, *Resonance Radiation and Excited Atoms*, Cambridge University Press, Cambridge, 1934.
6 L. F. Phillips, in K. R. Jennings and R. B. Cundall, (eds.), *Progress in Reaction Kinetics*, Vol. 7, Pergamon Press, London, 1973, p. 83.
7 L. F. Phillips, *Can. J. Chem.*, 51 (1973) 1517.
8 P. D. Morten, C. G. Freeman, R. F. C. Claridge and L. F. Phillips, to be published.